

## Tuning the Optical Gap of Nanometer-Size Diamond Cages by Sulfurization: A Time-Dependent Density Functional Study

Márton Vörös,<sup>1</sup> Tamás Demjén,<sup>2,3</sup> Tibor Szilvási,<sup>1,4</sup> and Adam Gali<sup>1,3</sup>

<sup>1</sup>Department of Atomic Physics, Budapest University of Technology and Economics, Budafoki út 8., H-1111, Budapest, Hungary

<sup>2</sup>Institute of Physics, Loránd Eötvös University, Pázmány Péter sétány 1/A, H-1117 Budapest, Hungary

<sup>3</sup>Institute for Solid State Physics and Optics, Wigner Research Center for Physics, Hungarian Academy of Sciences, P.O. Box 49, H-1525 Budapest

<sup>4</sup>Department of Inorganic and Analytical Chemistry, Budapest University of Technology and Economics, Szent Gellért tér 4., H-1111, Budapest, Hungary

(Received 22 February 2012; published 26 June 2012)

The optical gap of nanometer sized diamond cages, i.e., diamondoids, lies in the ultraviolet spectral region. Here we show by hybrid functional based time-dependent density-functional calculations that, by varying the number of C=S double bonds at the surface of diamondoids, the absorption onset can be tuned toward the infrared spectral region. Our finding has an important implication for *in vivo* biological applications where toxic and unstable dye molecules may be substituted by the luminescent sulfurized diamondoids.

DOI: [10.1103/PhysRevLett.108.267401](https://doi.org/10.1103/PhysRevLett.108.267401)

PACS numbers: 78.67.Bf, 36.40.Vz, 71.15.Qe, 73.22.-f

Small molecule-sized fluorescent emitters are needed as probes to image and track the locations of targeted nano-sized objects with minimal perturbation and are much sought after for applications ranging from novel materials development to probing protein interactions in living cells [1]. Dye molecules have a very high brightness per unit volume or mass but are inherently not photostable at room temperature. While there are attempts to develop photostable dye molecules for *in vivo* bioimaging [2], alternatively, quantum dots that exhibit the desired photostability may be applied instead [3,4]. The typical quantum dots need a thick outer passivation that brings the total size up to the 10 nm range. These quantum dots are about thousands of times heavier than typical dye molecules and the targeted molecules; thus, quantum dots may bias the normal operation of the studied (bio)molecules.

Smallest size diamond cages, i.e., diamondoids [5–8], have about the same size like typical dye molecules, and they contain exclusively  $sp^3$  C atoms, in contrast to dye molecules. Diamondoids are thus photostable at room temperature; however, the luminescence takes place in the ultraviolet region [9,10], which inhibits their application for *in vivo* bioimaging applications where infrared emission in the range of 700 to 1000 nm is desired. While increasing the size of these diamondoids increases the optical gap [9,11–13], it is still in the ultraviolet spectral region due to quantum confinement effects. Previous calculations and experiments showed that it may be possible to lower the optical gap of diamondoids by functionalization [14–17]; however, the infrared range is still far from being reached.

Diamondoids are hydrocarbon molecules where each carbon dangling bond at the surface is terminated by a hydrogen atom. Here we show by time-dependent

density-functional theory (TDDFT) calculations that if appropriate hydrogen atoms are subsequently substituted by sulfur atoms in the diamondoids then the first excitation energy of the diamondoids can be gradually shifted from the ultraviolet downward to the infrared spectral region. These sulfurized diamondoids may fulfill the stringent criteria of photostability, size, and range of emission for *in vivo* biomarker applications and may substitute the unstable dye molecules and the too large quantum dots.

We used the PWSCF code (part of the QUANTUM ESPRESSO package [18]) to calculate the ground-state geometries of the nanocrystals by employing the Perdew-Burke-Ernzerhof (PBE) functional [19] within DFT. Electron-nuclei interaction was handled by using standard ultrasoft pseudopotentials [20]. Wave functions were expanded using plane waves with a kinetic energy cutoff of 35 Ry, while the charge density with a 10 times larger cutoff, which is usually needed to carefully handle augmentation charges that arise in the ultrasoft scheme. In order to avoid the artificial nanocrystal-nanocrystal interaction, at least 1 nm vacuum was added to the cell in each spatial direction, which ensures good convergence in ground-state properties. All atoms were allowed to relax until Born-Oppenheimer forces became smaller than the given threshold. Excited-state calculations were carried out by the cluster code TURBOMOLE [21] in the TDDFT framework within the adiabatic approximation. We used the PBE0 hybrid functional [22] both in the ground- and excited-state calculations with a large augmented correlation-consistent polarized valence triple zeta basis set [23,24]. We applied this methodology in our earlier studies where we could obtain the experimental optical gaps with good accuracy ( $\leq 0.2$  eV) for hydrogenated diamondoids [25]. We used this tool to predict the optical gap of sulfurized diamondoids.

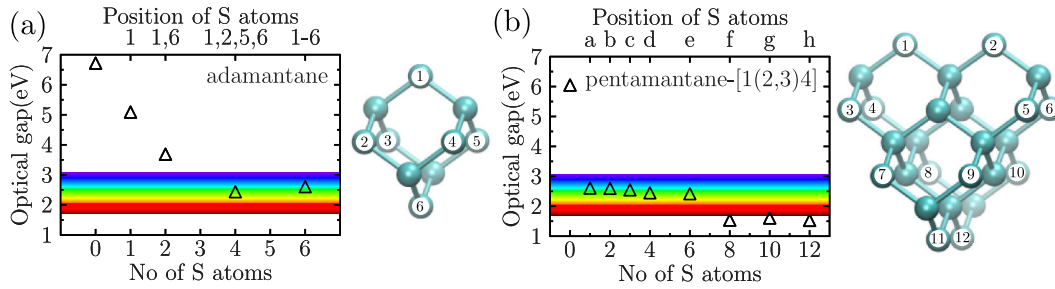


FIG. 1 (color online). The structures and the lowest energy excitations are shown for sulfurized (a) adamantane and (b) pentamantane [1(2,3)4] as a function of the number of  $=S$  double bonds at the surface. Cyan balls depict C atoms. Hydrogen atoms are not shown for clarity. The  $=S$  substitutions are indicated by numbers on the upper  $x$  axis of the plots for adamantane and by letters for pentamantane [1(2,3)4], where the dictionary for the letter-number correspondence is the following:  $a = 1$ ;  $b = 1, 12$ ;  $c = 1, 9, 10$ ;  $d = 1, 3, 10, 12$ ;  $e = 1, 4, 5, 7, 10, 11$ ;  $f = 1, 4, 5, 7-11$ ;  $g = 1-3, 6-12$ ;  $h = 1-12$ . These numbers on the structures next to the graphs represent C atoms to which S atoms bond.  $C=S$  double bonds are involved in the excitations. See text for more details.

We studied the smallest diamond cage, adamantane, and a larger one, pentamantane[1(2,3)4], that contain 10 and 32 C atoms, respectively (see Fig. 1). Some surface C atoms bond to two hydrogen atoms where the two H atoms may be substituted by a single sulfur atom, creating a double bond between the C and S atoms. We substituted 1, 2, 4, and 6 S atoms in adamantane while 1, 2, 3, 4, 6, 8, 10, and 12 S atoms in pentamantane[1(2,3)4] where we considered always the lowest energy configuration among the possible structures in the excitation calculations. Their calculated lowest energy transitions can be seen in Fig. 1.

As apparent, the calculated optical gaps are gradually decreasing with increasing number of thio groups on the surface of diamondoids. In adamantane, a maximum of six thio groups may be attached, while 12 sulfur atoms in pentamantane[1(2,3)4]. Accordingly, the reduction of the optical gap for pentamantane[1(2,3)4] is larger, and it eventually reaches the infrared spectral region. Adamantane with  $=S$  substitution of two H atoms has already been synthesized [26], and it is known as adamantanethione. Previous measurements indicated that  $=S$  functionalized adamantanes are stable in solution; in addition, in the presence of  $S-H$  functional groups it can form an  $S-S$  bond [27], which is one of the most common methods to immobilize the fluorescent agent, especially using quantum dots, on a biomolecule [28]. Therefore S-modified diamondoids can covalently bond to biomolecules similarly to quantum dots without passivation by its own nature, and the tracking of the location of the targeted biomolecule may be detected optically. The number of atoms in sulfurized pentamantane[1(2,3)4] is in the range of that of typical dye molecules but exhibits much stronger photostability due to the lack of extended aromatic systems; thus, we propose it as a good candidate for realizing *in vivo* biomarkers.

We note that experimental studies indicate that it may be indeed possible to fabricate diamondoids with more than one  $C=S$  double bond at the surface [29]. For example, adamantane with two  $C=S$  double bonds, adamantanethione, is a well-known structure synthesized by using

the corresponding ketone [29]. This transformation is also known as thionation and may be achieved by using thionation reagents, such as  $P_2S_5$  [29] or  $P_4S_{10}$  [30]. Since adamantane with three  $C=O$  bonds at the surface has already been produced [31], it is expected that higher coverage of higher diamondoids is also possible.

It is imperative to understand the nature of low-energy excitations in these structures. First, we analyze the single  $C=S$  double bond in adamantanethione as a case study in order to unravel its effect on the excitation spectrum. To our knowledge, this is the only structure among the proposed sulfurized diamondoids where the corresponding experimental absorption spectrum is available [30] and can be directly compared to our calculations. The highest occupied molecular orbital (HOMO) of the pristine adamantane with  $T_d$  symmetry originates from the bonding combination of  $sp^3$  bonds between C and H atoms ( $\sigma$  state), while the lowest unoccupied molecular orbital (LUMO) is a “superautom”  $3s$ -type Rydberg state [25,32] where the TDPBE0 gap (which is the short notation for the first dipole allowed optical transition calculated at the TDDFT level with the PBE0 functional) is about 6.7 eV. By substituting two hydrogen atoms with  $a = S$  bond, the symmetry is reduced to  $C_{2v}$  and the TDPBE0 gap is decreased down to 5.0 eV. The HOMO state is a lone pair on the S atom ( $n$  state), while the LUMO is the antibonding combination of the  $\pi$  bond between neighboring C and S atoms ( $\pi^*$  state). The bonding combination ( $\pi$  state) yields the HOMO  $- 1$  level (one state below HOMO in energy). However, the HOMO has  $b_2$  symmetry whereas LUMO has  $b_1$  symmetry, and the transition between these two states is dipole forbidden; thus, the HOMO-LUMO gap does not correspond to any dipole allowed optical transition. Instead, the 5.0 eV optical gap is obtained by the dipole allowed transition between HOMO and  $4s$ —where  $4s$  is a Rydberg state—LUMO  $+ 1$  (the nearest state above LUMO in energy). This is still significantly lower than that of pristine adamantane. See Fig. 2(a) for the projected density of states of this structure, showing that HOMO  $- 1$ , HOMO, and LUMO states have

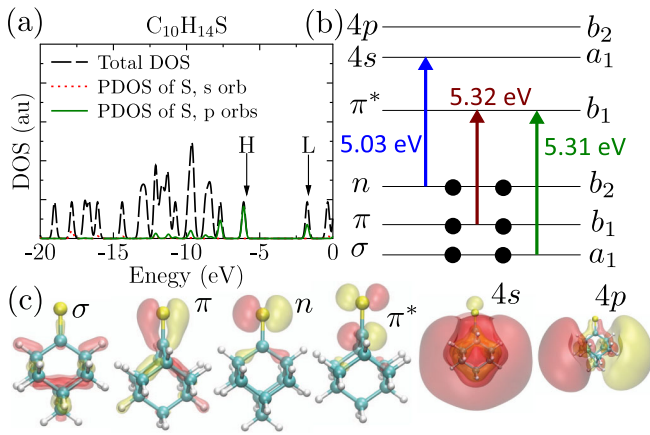


FIG. 2 (color online). (a) Total and projected density of states (PDOS) of adamantanethione are shown where H and L denote the HOMO and LUMO energies, respectively. The projected  $s$  and  $p$  orbitals of sulfur atoms are depicted by red dotted and green continuous lines, respectively. (b) Schematic diagram about the order of single particle states. On the left the localization of the molecular orbitals is labeled while the symmetry of these orbitals is shown on the right. The HOMO state is  $n(b_2)$  while the LUMO is  $\pi^*(b_1)$ . Arrows are representing the calculated lowest excitations between these states. The corresponding excitation energies are also given. (c) Adamantanethione structure: small white, larger cyan, and largest yellow balls depict H, C, and S atoms, respectively. The isovalue of the calculated wave functions are shown where red (dark gray) and yellow (light gray) colors represent the positive and negative values with the corresponding label of the molecular orbitals.

significant contributions from sulfur atomic orbitals and Figs. 2(b) and 2(c) for the ordering and isovalue surfaces of the single particle states. In the experiments it was claimed that the first optical transition is a  $\pi \rightarrow \pi^*$  transition with energy  $\approx 5.3$  eV, and the second lowest transition is a  $n \rightarrow 4s$  transition with energy 5.4 eV. The proximity of these two peaks suggests that there is a fine interplay between local (where local transition means that the spatial localization of the initial and final molecular orbitals is similar) and Rydberg-like excitations. Our calculations correctly describe the  $\pi \rightarrow \pi^*$  transition having an excitation energy of 5.3 eV; however, the Rydberg transition is underestimated by  $\approx 0.4$  eV. This discrepancy can be attributed to the long range behavior of the PBE0 functional [33]. Our findings of the calculated lowest energy peaks are summarized in Fig. 2(b). We note that Bader analysis [34] shows a slight positive polarization on the S atom and negative polarization on the C atom in the C=S double bond.

After justification of our methodology on experimentally known structures, we added more C=S double bonds in the adamantane cage in order to decrease the optical gap toward the desired energy range. Because the positively polarized S atoms repel each other, they sit the farthest in the most stable configurations. In the case of two C=S double bonds, the single particle levels close to the HOMO

and LUMO in energy are similar to those of adamantanethione. However, the symmetry is  $D_{2d}$ ; thus, the  $n \rightarrow \pi^*$  transition is dipole allowed. As a consequence, the optical gap is reduced to 3.6 eV, but it is still in the ultraviolet energy region. In the case of four C=S bonds, the symmetry is again  $D_{2d}$ , but the optical gap is 2.4 eV lying in the visible energy region. Interestingly, by introducing six C=S double bonds the optical gap does not reduce further but slightly increases up to 2.6 eV, which is still in the visible energy region. In these cases, the dependence of the HOMO-LUMO gap on the number of C=S double bonds correlates with the optical gap.

By adding more and more C=S double bonds, we found that the shape of the HOMO and LUMO wave functions do not change considerably; however, Bader analysis [34] showed that the charge transfer from the sulfur atoms toward carbon atoms increases. One may model the effect of neighboring C=S groups as a dipole with increasing charge on the given C=S double bond where the wave functions are localized. The effect of this dipole with a charge of  $\Delta \times e$  on the energies of HOMO and LUMO states may be described by first order perturbation theory. In this case, the correction to the states is:  $\langle \phi(r) | \Delta \frac{e^2}{4\pi\epsilon_0} \times (\frac{1}{|r-r_S|} - \frac{1}{|r-r_C|}) | \phi(r) \rangle$ , where  $r_S$  and  $r_C$  are the positions of the sulfur and carbon atoms, respectively, and  $\phi(r)$  is either the HOMO or LUMO state extracted from our *ab initio* calculations on adamantanethione. Shifts of the HOMO-LUMO gap calculated by this model are on the same order of magnitude as obtained from *ab initio* calculations and follow the trend closely [35]. This confirms that the main driving force of the gap reduction is the charge transfer, which is caused by the steric interaction between close sulfur atoms. This finding, together with the selection rule dictated by the symmetry of structures, explains the complex behavior of the gap dependence on the number of sulfur atoms. All in all, we demonstrated here that sulfurized adamantane may exhibit excitation energy in the visible energy range close to blue color that may serve as a biomarker.

Insight on the effect of C=S double bonds on the excitation spectrum inspired us to extend our investigations on sulfurized pentamantane[1(2,3)4] where the combination of C=S double bonds allows more play with the symmetry and the mixture of C=S related states than that in adamantane. Pentamantane[1(2,3)4] has  $T_d$  symmetry and contains only 32 C atoms, so its size is still comparable with that of dye molecules. For instance, one C=S double bond will lower the symmetry to  $C_{1h}$  and introduces  $n$  HOMO and  $\pi^*$  LUMO states. Because of the low symmetry the  $n \rightarrow \pi^*$  transition is dipole allowed, and one obtains 2.6 eV for the lowest excitation energy, which is a substantial decrease of the gap of 6.0 eV of the pure pentamantane[1(2,3)4]. Only by single C=S double bonds in pentamantane[1(2,3)4] one can achieve a visible emission. By introducing two, three, four, and six C=S

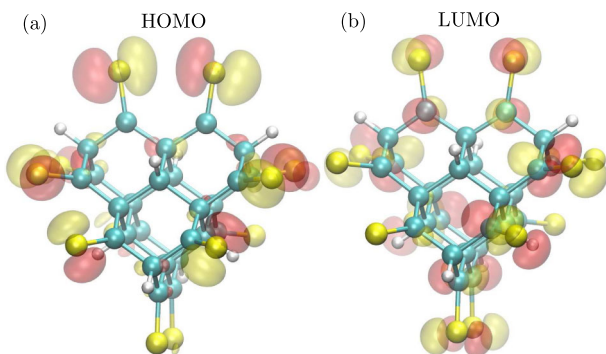


FIG. 3 (color online). Isovalue representation of the (a) HOMO and (b) LUMO states of 12 C=S double bonds in pentamantane[1(2,3)4] where red (dark gray) and yellow (light gray) colors represent positive and negative values of the corresponding molecular orbitals. Small white, larger cyan, and largest yellow balls depict H, C, and S atoms, respectively.

double bonds, there is no significant further redshift of the gap; e.g., the optical gap of pentamantane[1(2,3)4] with six C=S double bonds is 2.4 eV. This can be understood by the fact that in these cases the sulfur atoms sit relatively far away from each other with no steric interaction, which would result in additional charge transfer. However, as at least eight C=S double bonds are on the surface of pentamantane[1(2,3)4] close sulfur atoms repel each other, which results in a more pronounced charge transfer, causing the optical gap to decrease even further as our model described in the case of adamantane predicts. Finally, the lowest excitation energy is in the desired infrared energy region: it is 1.5 eV in the case of 12 C=S double bonds. The HOMO and LUMO states of this sulfurized diamondoid, responsible for the first dipole allowed transition, are shown in Fig. 3 where the strong interaction between close sulfur atoms is apparent. This is the basic driving force of the redshift in the excitation spectrum of sulfurized pentamantane[1(2,3)4].

In summary, we demonstrated by time-dependent density-functional theory calculations that sulfurized small diamondoids exhibit visible or infrared emission depending on the number C=S double bonds at the surface. Particularly, sulfurized pentamantane[1(2,3)4] is a very promising candidate for *in vivo* biomarker applications. We analyzed how the C=S double bonds redshift the optical gap, which might serve as a guide to find alternative solutions to existing fluorophores.

A. G. and M. V. acknowledge the support from the NIIF Supercomputer Center Grant No. 1090 and the NHDP TAMOP-4.2.1/B-09/1/KMR-2010-0002 program. A. G. also acknowledges the support from EU FP7 grant DIAMANT (Grant No. 270197).

[1] D. Evanko, *Nat. Methods* **5**, 218 (2008).

[2] T. M. S. Goncalves, *Chem. Rev.* **109**, 190 (2009).

- [3] V. Biju, T. Itoh, A. Anas, A. Sujith, and M. Ishikawa, *Anal. Bioanal. Chem.* **391**, 2469 (2008).
- [4] X. Michalet, F. F. Pinaud, L. A. Bentolila, J. M. Tsay, S. Doose, J. J. Li, G. Sundaresan, A. M. Wu, S. S. Gambhir, and S. Weiss, *Science* **307**, 538 (2005).
- [5] J. E. Dahl, S. G. Liu, and R. M. K. Carlson, *Science* **299**, 96 (2003).
- [6] A. A. Fokin, P. R. Schreiner, N. A. Fokina, B. A. Tkachenko, M. Serafin, J. E. P. Dahl, S. Liu, and R. M. K. Carlson, *J. Org. Chem.* **71**, 8532 (2006).
- [7] P. R. Schreiner, N. A. Fokina, B. A. Tkachenko, H. Hausmann, M. Serafin, J. E. P. Dahl, S. Liu, R. M. K. Carlson, and A. A. Fokin, *J. Org. Chem.* **71**, 6709 (2006).
- [8] H. Schwertfeger, A. A. Fokin, and P. R. Schreiner, *Angew. Chem., Int. Ed. Engl.* **47**, 1022 (2008).
- [9] L. Landt, K. Klunder, J. E. Dahl, R. M. K. Carlson, T. Moller, and C. Bostedt, *Phys. Rev. Lett.* **103**, 047402 (2009).
- [10] L. Landt, W. Kielich, D. Wolter, M. Staiger, A. Ehresmann, T. Möller, and C. Bostedt, *Phys. Rev. B* **80**, 205323 (2009).
- [11] N. D. Drummond, A. J. Williamson, R. J. Needs, and G. Galli, *Phys. Rev. Lett.* **95**, 096801 (2005).
- [12] F. Marsusi, J. Sabbaghzadeh, and N. D. Drummond, *Phys. Rev. B* **84**, 245315 (2011).
- [13] *Proceedings of the Europhysics Conference on Computational Physics Genoa, 2004*, edited by M. Ferrario, S. Melchionna, and C. Pierleoni [Comput. Phys. Commun. 169, No. 14 (2005)].
- [14] L. Landt, C. Bostedt, D. Wolter, T. Möller, J. E. P. Dahl, R. M. K. Carlson, B. A. Tkachenko, A. A. Fokin, P. R. Schreiner, A. Kulesza, R. Mitrić, and V. Bonacić-Koutecký, *J. Chem. Phys.* **132**, 144305 (2010).
- [15] L. Landt, M. Staiger, D. Wolter, K. Klunder, P. Zimmermann, T. M. Willey, T. van Buuren, D. Brehmer, P. R. Schreiner, B. A. Tkachenko, A. A. Fokin, T. Möller, and C. Bostedt, *J. Chem. Phys.* **132**, 024710 (2010).
- [16] A. Fokin and P. Schreiner, *Mol. Phys.* **107**, 823 (2009).
- [17] V. Petráková, A. Taylor, I. Kratochvílová, F. Fendrych, J. Vacík, J. Kučka, J. Štursa, P. Cígler, M. Ledvina, A. Fišerová, P. Kneppo, and M. Nesládek, *Adv. Funct. Mater.* **22**, 812 (2012).
- [18] P. Giannozzi *et al.*, *J. Phys. Condens. Matter* **21**, 395502 (2009).
- [19] J. P. Perdew, K. Burke, and M. Ernzerhof, *Phys. Rev. Lett.* **77**, 3865 (1996).
- [20] D. Vanderbilt, *Phys. Rev. B* **41**, 7892 (1990).
- [21] R. Ahlrichs, M. Bär, M. Häser, H. Horn, and C. Kölmel, *Chem. Phys. Lett.* **162**, 165 (1989).
- [22] J. P. Perdew, M. Ernzerhof, and K. Burke, *J. Chem. Phys.* **105**, 9982 (1996).
- [23] K. L. Schuchardt, B. T. Didier, T. Elsethagen, L. Sun, V. Gurumoorthi, J. Chase, J. Li, and T. L. Windus, *J. Chem. Inf. Model.* **47**, 1045 (2007).
- [24] While we applied a different functional in the geometry optimization (PBE) than in optical calculations (PBE0), tests on adamantane showed that this slight discrepancy results in an error of less than 0.05 eV for the excitation energies of interest, thus can be safely neglected.
- [25] M. Vörös and A. Gali, *Phys. Rev. B* **80**, 161411 (2009).

- [26] J. W. Greidanus and W. J. Schwalm, *Can. J. Chem.* **47**, 3715 (1969).
- [27] J. R. Bolton, K. S. Chen, A. H. Lawrence, and P. de Mayo, *J. Am. Chem. Soc.* **97**, 1832 (1975).
- [28] W. C. W. Chan and S. Nie, *Science* **281**, 2016 (1998).
- [29] S. Bernhard and P. Belser, *Synthesis* **1996**, 192 (1996).
- [30] K. J. Falk and R. P. Steer, *Can. J. Chem.* **66**, 575 (1988).
- [31] M. Giasuddin Ahmed, S. M. Iqbal Moeiz, S. Asghari Ahmed, M. Abu Hena, Y. Tsuda, and P. Sampson, *J. Chem. Res. (S)* **(1998)** 282.
- [32] J. W. Raymond, *J. Chem. Phys.* **56**, 3912 (1972).
- [33] C. Adamo, G. E. Scuseria, and V. Barone, *J. Chem. Phys.* **111**, 2889 (1999).
- [34] Bader analyses were calculated by the help of VASP code, using standard projectors to eliminate the core electrons at the optimized geometry obtained from PWSCF calculation.
- [35] In principle, the screened Coulomb interaction should be used to evaluate such a model picture. However, the screening in small nanocrystals approaches the vacuum limit; thus, approximating the screening by the screening of vacuum can be considered to be a good estimate.